ESAIM: M2AN 47 (2013) 401–420
DOI: 10.1051/m2an/2012032

ESAIM: Mathematical Modelling and Numerical Analysis
www.esaim-m2an.org

STABLE DISCRETIZATION OF A DIFFUSE INTERFACE MODEL FOR LIQUID-VAPOR FLOWS WITH SURFACE TENSION

Malte Braack[1] and Andreas Prohl[2]

Abstract. The isothermal Navier–Stokes–Korteweg system is used to model dynamics of a compressible fluid exhibiting phase transitions between a liquid and a vapor phase in the presence of capillarity effects close to phase boundaries. Standard numerical discretizations are known to violate discrete versions of inherent energy inequalities, thus leading to spurious dynamics of computed solutions close to static equilibria (*e.g.*, parasitic currents). In this work, we propose a time-implicit discretization of the problem, and use piecewise linear (or bilinear), globally continuous finite element spaces for both, velocity and density fields, and two regularizing terms where corresponding parameters tend to zero as the mesh-size $h > 0$ tends to zero. Solvability, non-negativity of computed densities, as well as conservation of mass, and a discrete energy law to control dynamics are shown. Computational experiments are provided to study interesting regimes of coefficients for viscosity and capillarity.

Mathematics Subject Classification. 65M60, 65M12, 76W05.

Received April 11, 2011. Revised March 10, 2012.
Published online January 11, 2013.

1. Introduction

We consider a compressible fluid contained in a bounded domain $\Omega \subset \mathbb{R}^d$, for $d = 2, 3$, which consists of both, liquid and vapor phases. A typical scenario are vapor bubbles in a liquid, which may oscillate, grow until they break up again, or disappear, where in the latter regime surface tension effects become increasingly important. The isothermal compressible Navier–Stokes–Korteweg (NSK) model describes liquid-vapor diffuse interfaces with surface tension (see [1, 8]).

Densities are non-negative, which is a relevant property of solutions of the NSK model. Another important feature of the NSK model is an energy identity which balances kinetic energy, Van-der-Waals free energy, viscous dissipation, and external forces. In different works [1, 5, 15, 20] focused on computationally solving the Korteweg system it is reported that computed solutions should satisfy a (discrete version) of the energy law. It is conjectured that observed numerical artefacts, *e.g.*, spurious 'parasitic currents' inside diffuse interfaces, occur for discretizations which violate a discrete energy law and/or non-negativity of computed densities. Recently,

Keywords and phrases. Diffuse interface model, surface tension, structure preserving discretization, space-time discretization.

[1] Mathematisches Seminar, Christian-Albrechts-Universität zu Kiel, Westring 393, 24098 Kiel, Germany.
braack@math.uni-kiel.de

[2] Mathematisches Institut, Universität Tübingen, Auf der Morgenstelle 10, 72076 Tübingen, Germany.
prohl@na.uni-tuebingen.de

different strategies have been proposed to address this problem. Computational studies in *e.g.* [5,15] obtain non-negative density iterates, and a decay of energies to reliably approximate equilibria. However, no theoretical results are provided to justify these observations. It is the goal of this work to construct a finite element based space-time discretization of the NSK model, where:

- density iterates are shown to conserve mass;
- densities stay non-negative;
- and iterates satisfy a (perturbed) discrete version of the energy law.

Constructing such a scheme is nontrivial, since nonlinear test functions of density and velocity are needed in the derivation of the mentioned energy law and such test functions are usually not admitted in finite element discretizations.

This work is organized as follows: in Section 2 we present the Navier–Stokes–Korteweg model and the energy law mentioned above. Section 3 provides detailed arguments leading to the system which is equivalent to NSK, and a proper starting point for constructing stable numerical schemes. In Section 4, necessary technical tools are collected and the numerical scheme is given. Mass conservation, non-negativity of densities, as well as a discrete energy law for iterates are derived in Theorem 4.4. Finally, computational studies are reported in Section 5.

2. Navier–Stokes–Korteweg model

As usual in fluid dynamics, we use the notation ρ for the density of the fluid, $\mathbf{u}$ as velocity field, $\mathbf{f}$ as external forces, and T as final time. The Navier–Stokes–Korteweg (NSK) model reads (see [1,5,7,8])

$$\rho_t + \operatorname{div}\big(\rho\mathbf{u}\big) = 0 \qquad \text{in } \Omega_T := (0,T)\times\Omega, \tag{2.1}$$

$$\big(\rho\mathbf{u}\big)_t + \operatorname{div}\big(\rho\mathbf{u}\otimes\mathbf{u}\big) - \operatorname{div}\big(\mathbf{S}+\mathbf{K}\big) = \rho\mathbf{f} \qquad \text{in } \Omega_T\,, \tag{2.2}$$

$$\frac{\partial\rho}{\partial\mathbf{n}} = 0, \qquad \mathbf{u} = \mathbf{0} \qquad \text{on } \partial\Omega_T := (0,T)\times\partial\Omega, \tag{2.3}$$

$$\rho(0,\cdot) = \rho_0 \geq 0, \qquad \big(\rho\mathbf{u}\big)(0,\cdot) = \mathbf{m}_0 \qquad \text{in } \Omega\,, \tag{2.4}$$

where the (standard) total stress tensor $\mathbf{S} : \Omega_T \to \mathbb{R}^{d\times d}_{\mathrm{sym}}$, and the Korteweg stress tensor $\mathbf{K} : \Omega_T \to \mathbb{R}^{d\times d}_{\mathrm{sym}}$ accounting for capillarity effects of the diffuse vapor-liquid interface read as

$$\mathbf{S} = 2\mu\mathbf{D}(\mathbf{u}) + \big(\lambda\operatorname{div}\mathbf{u} - P(\rho)\big)\mathbf{I}, \tag{2.5}$$

$$\mathbf{K} = \kappa\Big[\big(\rho\Delta\rho + \frac{|\nabla\rho|^2}{2}\big)\mathbf{I} - \nabla\rho\otimes\nabla\rho\Big]. \tag{2.6}$$

Here, $\mathbf{D}(\mathbf{u})_{ij} = \frac{1}{2}\big(\partial_i u_j + \partial_j u_i\big)$ is the symmetric strain tensor, $\lambda,\mu > 0$ are constant viscosity coefficients, and $\kappa > 0$ is the coefficient of capillarity. The pressure is denoted by P and depends on the density by an algebraic correlation. The expressions ρ_0 and $\mathbf{m_0}$ are initial density and momentum, respectively.

2.1. Phase transition

The density ρ plays the role as an order parameter that distinguishes both, liquid and vapor phase, which are separated by an intervening interface: for regions where no phase transitions take place, the model approximates the compressible Navier–Stokes system; places where ρ changes rapidly assemble the diffuse interface, and the Korteweg tensor $\mathbf{S}$ gives nontrivial contributions here to model capillarity effects. For the capillarity force in (2.2), we calculate

$$\operatorname{div}\mathbf{K} = \kappa\rho\nabla\Delta\rho. \tag{2.7}$$

The pressure $P : [0,b) \to (0,\infty)$ is a given function of Van-der-Waals type (see Fig. 1, right) of the density serving as order-parameter, to properly cover both, the pressure in the 'low density'/vapor phase, and the 'high

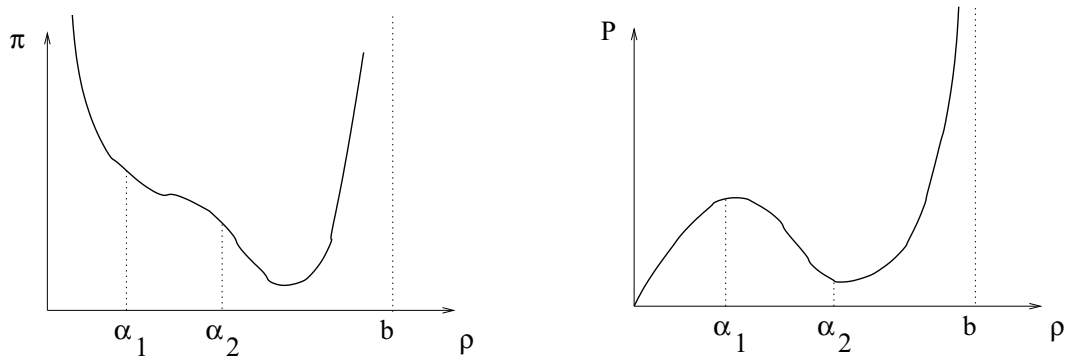

FIGURE 1. Nonconvex energy π (left), and non-monotone pressure function P (right).

density'/liquid phase, see *e.g.* [7],

$$P(\rho) = \frac{a\rho}{b-\rho} - \rho^2 \qquad (a, b > 0). \tag{2.8}$$

Let $0 < \alpha_1 < \alpha_2 < b$ be those values where $P'(\alpha_1) = P'(\alpha_2) = 0$, and $P''(\alpha_1) < 0$, $P''(\alpha_2) > 0$. We may then define different phases: if the density ρ lies in the interval $[0, \alpha_1]$, the corresponding fluid state is 'vapor', and it is 'liquid' if $\rho \in [\alpha_2, b)$; the non-physical, spinodal state where $\rho \in (\alpha_1, \alpha_2)$ is often referred to as 'elliptic'; see [5, 19] for further details.

2.2. Existence of solutions

We conclude the setup of the problem with some remarks concerning solvability of (2.1)–(2.6): Local existence of regular solutions to the Cauchy problem (2.1)–(2.6) for constant coefficients and smooth initial data is shown in [13], and extended to Lipschitz continuous μ, λ, κ, and more general initial data in the setting of an IBVP in the recent work [17]; moreover, results in [13] are complemented in the same setting by the work [14] which shows global smooth solutions in the case of small smooth initial data. The results of [7] comprise global solutions for sufficiently small data and initial data close enough to stable equilibria, and local well-posedness for initial densities bounded away from zero in particular. Further extensions which address global existence of weak solutions for small initial data and specific choices of capillarity coefficients and general viscosity coefficients can be found in [12]. In [3], global weak solutions for (2.1)–(2.6), in the case $\mu \equiv \mu(\rho) = \nu\rho$ for $\nu > 0$, and $\lambda(\rho) = 0$ are constructed in a periodic or strip domain. The choice of these specific coefficients allows an estimate for $\rho \in L^2\big(0, T; W^{2,2}\big)$, using the standard Sobolev space notation. This is the key to pass to the limit in the given quadratic nonlinear capillarity term. To reliably cope with places where vacuum occurs, *i.e.*, where information on the velocity $\mathbf{u}$ is lost, an adopted weak formulation of (2.2) is chosen to reflect this issue.

2.3. Energy law

Classical solutions of the Korteweg system (2.1)–(2.6) conserve initial mass, and have nonnegative densities $\rho(t, \cdot) \geq 0$ at all times $t \geq 0$, where the latter property follows from a simple calculation for ρ along characteristics (see *e.g.* [10], p. 43).

The pressure can be described by means of the energy potential $\pi : [0, b) \to \mathbb{R}^+$, and the following thermodynamic relation, see *e.g.* [7],

$$\pi(\rho) = \pi_0 + \rho \int_{\overline{\rho}}^{\rho} \frac{P(s)}{s^2} \mathrm{d}s - P(\overline{\rho})\frac{\rho}{\overline{\rho}},$$

where $\overline{\rho} > 0$ is a constant (and arbitrary) reference density. The constant π_0 is chosen in order to ensure $\pi > 0$. By partial fraction decomposition, the use of (2.8) and some basic calculus, π can also be expressed in the form

$$\pi(\rho) = \pi_0 + \frac{a}{b}\rho \ln\left(\frac{(b-\overline{\rho})\rho}{(b-\rho)\overline{\rho}}\right) + \rho\left(\overline{\rho} - \rho - \frac{P(\overline{\rho})}{\overline{\rho}}\right).$$

Moreover, the pressure can be expressed in terms of π and π':

$$P(\rho) = \rho\pi'(\rho) - \pi(\rho) - \pi_0. \tag{2.9}$$

We calculate

$$\nabla P(\rho) = \nabla\Big[\rho\pi'(\rho) - \pi(\rho)\Big] = \rho\nabla\pi'(\rho) + \pi'(\rho)\nabla\rho - \nabla\pi(\rho) = \rho\nabla\pi'(\rho). \tag{2.10}$$

Using (2.7) and (2.10), the momentum equation (2.2) can be reformulated as

$$\big(\rho\mathbf{u}\big)_t + \operatorname{div}\big(\rho\mathbf{u}\otimes\mathbf{u}\big) - 2\mu\operatorname{div}\big(\mathbf{D}(\mathbf{u})\big) - \lambda\nabla\big(\operatorname{div}\mathbf{u}\big) + \rho\nabla\Big(\pi'(\rho) - \kappa\boldsymbol{\Delta}\rho\Big) = \rho\mathbf{f}. \tag{2.11}$$

In order to include phase transition phenomena, we allow P to be non-monotone, and $P' \geq -c_0$, for some $c_0 > 0$.

Connected to the Navier–Stokes–Korteweg system are the kinetic energy W_{kin}, the Van-der-Waals free energy W_{VdW}, the dissipation terms W_{diss}, and the total energy W which assembles the previous two parts:

$$\begin{aligned}
W_{\mathrm{kin}}(\rho,\mathbf{u}) &= \frac{1}{2}\int_\Omega \rho|\mathbf{u}|^2\,\mathrm{d}\mathbf{x},\\
W_{VdW}(\rho,\nabla\rho) &= \int_\Omega \pi(\rho)\,\mathrm{d}\mathbf{x} + \frac{\kappa}{2}\|\nabla\rho\|^2,\\
W_{\mathrm{diss}}(\mathbf{u}) &= \int_\Omega \Big[2\mu\|\mathbf{D}(\mathbf{u})\|_F^2 + \lambda|\operatorname{div}\mathbf{u}|^2\Big]\,\mathrm{d}\mathbf{x},\\
W \equiv W\big(\rho,\nabla\rho,\mathbf{u}\big) &= W_{\mathrm{kin}}(\rho,\mathbf{u}) + W_{VdW}(\rho,\nabla\rho).
\end{aligned}$$

Here we use the notation $\|\cdot\|$ for the $L^2(\Omega)$-norm and $\|\cdot\|_F$ for the Frobenius norm, respectively. The standard $L^2(\Omega)$-inner product will be denoted by $(\cdot,\cdot)$. The following identity that employs differentiable functions $\mathbf{w} : \Omega \to \mathbb{R}^d$ will be used below,

$$\begin{aligned}
\big(\rho\big[\mathbf{u}\cdot\nabla\big]\mathbf{w},\mathbf{u}\big) + \big(\operatorname{div}\big[\rho\mathbf{u}\otimes\mathbf{u}\big],\mathbf{w}\big) &= \sum_{i,j=1}^{d}\Big(\big(\rho u_i\partial_i w_j, u_j\big) - \big(\rho u_j u_i, \partial_i w_j\big)\Big)\\
&= \sum_{i,j=1}^{d}\Big(\rho u_i, u_j\partial_i w_j - u_j\partial_i w_j\Big) = 0.
\end{aligned} \tag{2.12}$$

Solutions of the Navier–Stokes–Korteweg system satisfy the following energy identity:

Proposition 2.1. *Classical solutions of the NSK system satisfy*

$$\frac{\mathrm{d}W}{\mathrm{d}t} + W_{\mathrm{diss}}(\mathbf{u}) = \int_\Omega \rho\langle\mathbf{f},\mathbf{u}\rangle\,\mathrm{d}\mathbf{x}. \tag{2.13}$$

Proof. We multiply (2.11) with $\mathbf{u}$, integrate in space, and use the identities

$$\big((\rho\mathbf{u})_t,\mathbf{u}\big) = \big(\rho\mathbf{u}_t + \rho_t\mathbf{u},\mathbf{u}\big) = \frac{1}{2}\frac{\mathrm{d}}{\mathrm{d}t}\big(\rho,|\mathbf{u}|^2\big) + \frac{1}{2}\big(\rho_t,|\mathbf{u}|^2\big), \tag{2.14}$$

$$\Big(\operatorname{div}\big(\rho\mathbf{u}\otimes\mathbf{u}\big),\mathbf{u}\Big) = -\Big(\rho[\mathbf{u}\cdot\nabla]\mathbf{u},\mathbf{u}\Big) = \frac{1}{2}\big(\operatorname{div}(\rho\mathbf{u}),|\mathbf{u}|^2\big), \tag{2.15}$$

thanks to (2.12), where $|\mathbf{u}|^2 = \sum_{i=1}^d |u_i|^2$. This yields

$$\frac{1}{2}\frac{\mathrm{d}}{\mathrm{d}t}\big(\rho, |\mathbf{u}|^2\big) + 2\mu \left\| \|\mathbf{D}(\mathbf{u})\|_F \right\|^2 + \lambda \left\| \operatorname{div} \mathbf{u} \right\|^2 + \Big(\rho\mathbf{u}, \nabla[\pi'(\rho) - \kappa\Delta\rho]\Big) = \big(\rho\mathbf{f}, \mathbf{u}\big) - \frac{1}{2}\Big(\rho_t + \operatorname{div}(\rho\mathbf{u}), |\mathbf{u}|^2\Big). \quad (2.16)$$

Due to (2.1) the last term in (2.16) vanishes. Now, we use again (2.1), $(2.3)_1$, and the chain rule to conclude for the remaining term in (2.16)

$$\Big(\rho\mathbf{u}, \nabla[\pi'(\rho) - \kappa\Delta\rho]\Big) = \big(\rho_t, \pi'(\rho) - \kappa\Delta\rho\big) = \frac{\mathrm{d}}{\mathrm{d}t}\pi(\rho) + \frac{\kappa}{2}\frac{\mathrm{d}}{\mathrm{d}t}\|\nabla\rho\|^2, \quad (2.17)$$

which requires to multiply (2.1) with $\pi'(\rho) - \kappa\Delta\rho$, and integrate in space then. □

In order to derive a discrete version of the energy law we will introduce some regularizations of the NSK model as reported in the next section.

3. Regularization and reformulation of the Korteweg system

We start with the following regularized Korteweg system,

$$\rho_t + \operatorname{div}\big(\rho\mathbf{u}\big) - \alpha\Delta\rho = 0 \qquad \text{in } \Omega_T, \quad (3.1)$$

$$(\rho\mathbf{u})_t + \operatorname{div}\big(\rho\mathbf{u}\otimes\mathbf{u}\big) - 2\mu\operatorname{div}\big(\mathbf{D}(\mathbf{u})\big) - \lambda\nabla\big(\operatorname{div}\mathbf{u}\big)$$

$$-\frac{\alpha}{2}\mathbf{u}\Delta\rho - \gamma\operatorname{div}\big(\mathbf{D}(\mathbf{u}_t)\big) + \rho\nabla w = \rho\mathbf{f} \qquad \text{in } \Omega_T, \quad (3.2)$$

$$w - \pi'_\beta(\rho) + \kappa\Delta\rho = 0 \qquad \text{in } \Omega_T, \quad (3.3)$$

$$\frac{\partial\rho}{\partial\mathbf{n}} = 0, \qquad \mathbf{u} = \mathbf{0} \qquad \text{on } \partial\Omega_T, \quad (3.4)$$

$$\rho(0,\cdot) = \rho_0 \geq 0, \qquad \big(\rho\mathbf{u}\big)(0,\cdot) = \mathbf{m}_0 \qquad \text{in } \Omega. \quad (3.5)$$

This formulation involves regularizing terms $-\alpha\Delta\rho$, as well as $-\frac{\alpha}{2}\mathbf{u}\Delta\rho$ and $-\gamma\operatorname{div}\big(\mathbf{D}(\mathbf{u}_t)\big)$, where $\alpha, \gamma \geq 0$; moreover, an auxiliary variable w is employed, that uses the truncated term $\pi'_\beta(\rho)$ with a parameter $\beta > 0$ defined below. Weak solutions to (3.1)–(3.5) for $\alpha > 0$ may be constructed by a general Galerkin method, because of the a priori estimate for $\rho \in L^2(0,T;W^{2,2})$ in Lemma 3.1 below, which allows to pass to the limit in the most critical capillarity term. Passing to the limit $\alpha \to 0$ to hopefully recover (2.1)–(2.4) has to remain as an open problem at this place.

The principal ideas for introducing the additional terms and the modifications in (3.1)–(3.5) are as follows:

3.1. Additional Laplacians

In order to derive a M-matrix property of the system matrix related to a space-time discretization of (2.2) we have introduced in (3.1) the Laplacian of density, $-\alpha\Delta\rho$, with a non-negative parameter $\alpha \geq 0$ that later depends on the spatial mesh size h. For $h \to 0$ it holds $\alpha \to 0$.

It turns out, that bounds for velocity iterates are needed in stronger norms than those used in (2.13). To overcome this problem in a finite element setting, the further stabilization term $-\gamma\operatorname{div}\big(\mathbf{D}(\mathbf{u}_t)\big)$ is added in (3.2). Details of this argumentation, which requires a bootstrapping argument to finally validate non-negativity for computed density iterates for small enough $h > 0$, and proper values of α, γ are provided in Section 4.

3.2. Truncation of the energy function

The potential π_β is a truncation of the non-convex function π, which is needed in Section 4 to compensate for the missing chain rule in a space-time discrete setting. For every $\beta > \beta_0 = \|\pi'\|_{L^\infty(\alpha_1,\alpha_2)}$ there exist $r^1_\beta \in (0, \alpha_1)$

and $r_\beta^2 \in (\alpha_2, \infty)$ such that $-\pi'(r_\beta^1) = \pi'(r_\beta^2) = \beta$. We define $\pi'_\beta : \mathbb{R} \to \mathbb{R}$ *via*

$$\pi'_\beta(s) = \begin{cases} \pi'(s) & \text{if } s \in [r_\beta^1, r_\beta^2], \\ -\beta & \text{if } s \in (-\infty, r_\beta^1), \\ \beta & \text{if } s \in (r_\beta^2, \infty). \end{cases} \tag{3.6}$$

Consequently,

$$\pi_\beta(s) = \pi(r_\beta^1) + \int_{r_\beta^1}^{s} \pi'_\beta(y)\mathrm{d}y \qquad (s \geq r_\beta^1). \tag{3.7}$$

By construction, π_β is identical to π on $[r_\beta^1, r_\beta^2]$ and in particular in the non-convex regime (α_1, α_2).

3.3. Introduction of an auxiliary variable

To conclude (2.17), we previously multiplied the continuity equation with $\pi'(\rho) - \kappa\Delta\rho$. This step is not possible for a finite element formulation, because this is a nonlinear function of ρ, and because the discrete density will not be H^2-regular. To overcome the latter problem of second derivatives for the density we use a mixed approach; in order to mimic the chain rule in a time-discrete setting, we use a discrete derivative of the truncation π'_β. This aspect leads to the additional scalar variable w and to equation (3.3). Due to (2.9), π' (and its truncation π'_β) can in (3.3) be expressed in terms of ρ:

$$\pi'(\rho) = \frac{1}{\rho}\Big(\pi(\rho) - \pi_0 + P(\rho)\Big) \;=\; \frac{a}{b}\ln\left(\frac{\rho(b-\overline{\rho})}{\overline{\rho}(b-\rho)}\right) - \frac{P(\overline{\rho})}{\overline{\rho}} + \frac{P(\rho)}{\rho} - \rho + \overline{\rho}.$$

Later we will use also the second derivative of π:

$$\pi''(\rho) = \frac{P'(\rho)}{\rho}. \tag{3.8}$$

3.4. Energy estimate of the regularized system

The regularized Korteweg system (3.1)–(3.5) allows for a modified energy law as stated in the next Lemma.

Lemma 3.1. *A classical solution of the regularized NSK system (3.1)–(3.5) fulfills the energy law*

$$\begin{aligned} &\frac{\mathrm{d}}{\mathrm{d}t}\Big(W_{\mathrm{kin}}(\rho,\mathbf{u}) + W_{VdW,\beta}(\rho,\nabla\rho) + \frac{\gamma}{2}\|\|\mathbf{D}(\mathbf{u})\|_F\|^2\Big) \\ &\qquad + W_{\mathrm{diss}}(\mathbf{u}) + \alpha\kappa\|\Delta\rho\|^2 + \alpha\int_\Omega \pi''_\beta(\rho)|\nabla\rho|^2\,\mathrm{d}\mathbf{x} = \int_\Omega \rho\langle\mathbf{f},\mathbf{u}\rangle\,\mathrm{d}\mathbf{x}\,, \end{aligned}$$

where $W_{VdW,\beta}$ is defined as W_{VdW} with π being replaced by π_β:

$$W_{VdW,\beta}(\rho,\nabla\rho) := \int_\Omega \pi_\beta(\rho)\,\mathrm{d}\mathbf{x} + \frac{\kappa}{2}\,\|\nabla\rho\|^2.$$

Proof. We may follow the steps in the proof of Proposition 2.1 to verify the energy law. In a first step, we multiply (3.2) by $\mathbf{u}$ and integrate in space. Thanks to (2.14), (2.15), and (3.1) to be multiplied by $\frac{|\mathbf{u}|^2}{2}$, we find

$$\Big([\rho\mathbf{u}]_t + \mathrm{div}\big(\rho\mathbf{u}\otimes\mathbf{u}\big) - \frac{\alpha}{2}\Delta\rho\mathbf{u},\mathbf{u}\Big) = \frac{1}{2}\frac{\mathrm{d}}{\mathrm{d}t}\big(\rho,|\mathbf{u}|^2\big) + \frac{1}{2}\Big(\rho_t + \mathrm{div}(\rho\mathbf{u}) - \alpha\Delta\rho,|\mathbf{u}|^2\Big) = \frac{1}{2}\frac{\mathrm{d}}{\mathrm{d}t}\big(\rho,|\mathbf{u}|^2\big).$$

There remains to control the term $\big(\rho\nabla w,\mathbf{u}\big) = -\big(w,\mathrm{div}[\rho\mathbf{u}]\big)$. By using (3.1) after multiplication with w, as well as (3.3) after multiplication by ρ_t, resp. $-\Delta\rho$, we obtain

$$\begin{aligned} -\big(w,\mathrm{div}[\rho\mathbf{u}]\big) &= \big(w,\rho_t - \alpha\Delta\rho\big) = \big(w,\rho_t\big) - \alpha\Big(\pi'_\beta(\rho) - \kappa\Delta\rho,\Delta\rho\Big) \\ &= \frac{\mathrm{d}}{\mathrm{d}t}\left[\int_\Omega \pi_\beta(\rho)\,\mathrm{d}\mathbf{x} + \frac{\kappa}{2}\|\nabla\rho\|^2\right] + \alpha\left[\int_\Omega \pi''_\beta(\rho)|\nabla\rho|^2\,\mathrm{d}\mathbf{x} + \kappa\|\Delta\rho\|^2\right]. \end{aligned}$$

□

Remark 3.2. The last term on the left-hand side of the energy identity in Lemma 3.1 may change sign, since the regularized energy potential π_β is admitted to be non-convex. In particular, $\pi''_\beta(\rho) = \pi''(\rho) < 0$ for $\rho \in (\alpha_1, \alpha_2)$. Because of (3.8) and the following lines, we may conclude

$$\left| \alpha \int_{\Omega_{nc}} \pi''_\beta(\rho) |\nabla \rho|^2 \, \mathrm{d}\mathbf{x} \right| \leq \frac{\alpha c_0}{\alpha_1} \int_\Omega |\nabla \rho|^2 \, \mathrm{d}\mathbf{x} \leq \frac{2\alpha c_0}{\alpha_1 \kappa} W_{VdW,\beta}(\rho, \nabla \rho),$$

for the non-convex part $\Omega_{nc}(t) := \{\mathbf{x} \in \Omega : \rho(t, \mathbf{x}) \in (\alpha_1, \alpha_2)\}$, and $c_0 := \max\{|P'(\rho)| : \alpha_1 \leq \rho \leq \alpha_2\}$. Now, an upper bound for the energy at all finite times $T > 0$ follows by a Gronwall argument ($\mathbf{f} \equiv \mathbf{0}$):

$$\max_{0 \leq t \leq T} \Big(W_{\mathrm{kin}}(\rho, \mathbf{u}) + W_{VdW,\beta}(\rho, \nabla \rho) + \frac{\gamma}{2} \|\|\mathbf{D}(\mathbf{u})\|_F\|^2 \Big) + \int_0^T \Big(W_{\mathrm{diss}}(\mathbf{u}) + \alpha\kappa \|\Delta \rho\|^2 \Big) \, \mathrm{d}t \leq C_1 \exp(C_2 T),$$

with non-negative constants $C_1 \equiv W_{\mathrm{kin}}(\rho_0, \mathbf{u}_0) + W_{VdW,\beta}(\rho_0, \nabla \rho_0) + \frac{\gamma}{2} \|\mathbf{D}(\mathbf{u}_0)\|^2$, and $C_2 \equiv \frac{2\alpha}{\kappa} \frac{c_0}{\alpha_1}$.

This estimate evidences practical choices $\alpha \ll \kappa$ to ensure $\exp\big(C_2 T\big) \approx 1$ for finite times $T > 0$. See also Remark 4.2, where corresponding mesh-constraints for the related discretization scheme are derived, which guarantee a proper balancing of both, capillarity and regularization effects in the scheme.

3.5. Variational formulation of the regularized NSK system

The Proof of Lemma 3.1 uses non-linear functions of ρ to validate an energy law for (3.1)–(3.5). In the following, we use the continuity equation in the momentum equation to find a reformulation of the problem that allows for linear (test) functions of ρ to show stability. As a consequence, this version of the regularized NSK system will later turn out to be suitable for constructing a stable finite-element based discretization. This idea was proposed in [18] in a different context.

Lemma 3.3. *Let $(\rho, \mathbf{u})$ be a classical solution of the regularized equations (3.1) and (3.3). Then $(\rho, \mathbf{u})$ fulfils (3.2) iff*

$$\frac{1}{2} \Big(\rho \mathbf{u}_t + [\rho \mathbf{u}]_t + \rho [\mathbf{u} \cdot \nabla] \mathbf{u} + \operatorname{div}\big(\rho \mathbf{u} \otimes \mathbf{u}\big) \Big) - 2\mu \operatorname{div}\big(\mathbf{D}(\mathbf{u})\big) - \lambda \nabla \big(\operatorname{div} \mathbf{u}\big) - \gamma \operatorname{div}\big(\mathbf{D}(\mathbf{u}_t)\big) + \rho \nabla w = \rho \mathbf{f}. \tag{3.9}$$

In other words, (3.9) replaces (3.2) in the combination with (3.1) and (3.3), and skips the regularizing term $-\frac{\alpha}{2} \Delta \rho \mathbf{u}$.

Proof. For the i-th component we conclude

$$\begin{aligned} \Big(\operatorname{div}\big(\rho \mathbf{u} \otimes \mathbf{u}\big) \Big)_i &= \sum_{j=1}^d \partial_j \Big(\rho \mathbf{u} \otimes \mathbf{u} \Big)_{ij} = \sum_{j=1}^d \partial_j \Big(\rho u_i u_j \Big) = \sum_{j=1}^d \partial_j \Big(\rho u_j \Big) u_i + \sum_{j=1}^d \rho u_j \partial_j u_i \\ &= \operatorname{div}\big(\rho \mathbf{u}\big) u_i + \rho \big[\mathbf{u} \cdot \nabla\big] u_i. \end{aligned}$$

Together with (3.1), is equivalent to

$$\operatorname{div}\big(\rho \mathbf{u} \otimes \mathbf{u}\big) = \operatorname{div}\big(\rho \mathbf{u}\big) \mathbf{u} + \rho \big[\mathbf{u} \cdot \nabla\big] \mathbf{u} = -\big(\rho_t - \alpha \Delta \rho\big) \mathbf{u} + \rho \big[\mathbf{u} \cdot \nabla\big] \mathbf{u},$$

which yields to

$$[\rho \mathbf{u}]_t + \operatorname{div}\big(\rho \mathbf{u} \otimes \mathbf{u}\big) = \rho \mathbf{u}_t + \rho \big[\mathbf{u} \cdot \nabla\big] \mathbf{u} + \alpha \mathbf{u} \Delta \rho. \tag{3.10}$$

As a consequence, (3.10) then leads to

$$\begin{aligned} [\rho \mathbf{u}]_t + \operatorname{div}\big(\rho \mathbf{u} \otimes \mathbf{u}\big) - \frac{\alpha}{2} \mathbf{u} \Delta \rho &= \frac{1}{2} \Big(\rho \mathbf{u}_t + \rho \big[\mathbf{u} \cdot \nabla\big] \mathbf{u} + \alpha \Delta \rho \mathbf{u} + [\rho \mathbf{u}]_t + \operatorname{div}\big(\rho \mathbf{u} \otimes \mathbf{u}\big) \Big) - \frac{\alpha}{2} \mathbf{u} \Delta \rho \\ &= \frac{1}{2} \Big(\rho \mathbf{u}_t + \rho \big[\mathbf{u} \cdot \nabla\big] \mathbf{u} + [\rho \mathbf{u}]_t + \operatorname{div}\big(\rho \mathbf{u} \otimes \mathbf{u}\big) \Big). \end{aligned}$$

Inserting this identity into (3.3) leads to (3.9). □

By (2.12), the weak form of the reformulated regularized NSK system (3.1), (3.9), (3.3)–(3.5) then is

$$\big(\rho_t,\chi\big) - \big(\rho\mathbf{u},\nabla\chi\big) + \alpha\big(\nabla\rho,\nabla\chi\big) = 0 \qquad \forall\,\chi\in C^\infty(\Omega), \tag{3.11}$$

$$\begin{aligned}&\frac{1}{2}\Big(\big(\rho\mathbf{u}_t,\mathbf{v}\big) + \big([\rho\mathbf{u}]_t,\mathbf{v}\big) + \big(\rho[\mathbf{u}\cdot\nabla]\mathbf{u},\mathbf{v}\big) - \big(\rho[\mathbf{u}\cdot\nabla]\mathbf{v},\mathbf{u}\big)\Big)\\ &+2\mu\big(\mathbf{D}(\mathbf{u}),\mathbf{D}(\mathbf{v})\big) + \lambda\big(\operatorname{div}\mathbf{u},\operatorname{div}\mathbf{v}\big) + \gamma\big(\mathbf{D}(\mathbf{u}_t),\mathbf{D}(\mathbf{v})\big) + \big(\rho\nabla w,\mathbf{v}\big) = \big(\rho\mathbf{f},\mathbf{v}\big) \quad \forall\,\mathbf{v}\in\mathbf{C}_0^\infty(\Omega),\end{aligned} \tag{3.12}$$

$$\big(w,\xi\big) - \big(\pi_\beta'(\rho),\xi\big) - \kappa\big(\nabla\rho,\nabla\xi\big) = 0 \qquad \forall\,\xi\in C^\infty(\Omega), \tag{3.13}$$

$$\rho(0,\cdot) = \rho_0, \qquad \big(\rho\mathbf{u}\big)(0,\cdot) = \mathbf{m}_0. \tag{3.14}$$

Taking the triple $\big(\chi,\mathbf{v},\xi\big) = \big(w,\mathbf{u},-\Delta\rho\big)$, and also $\xi=\rho_t$ in (3.13) then leads to the energy identity in Lemma 3.1. A stable discretization of (3.11)–(3.14) in space and time will be presented in Section 4.

4. Stable discretization of the regularized Korteweg system

4.1. Preliminaries

For the discretization we restrict to polygonal domains Ω. We consider quasi-uniform triangulations $\mathcal{T}_h$ of the domain $\Omega\subset\mathbb{R}^d$ into simplices or quadrilaterals/hexaedrals (but not both together) of maximal diameter $h>0$, *i.e.*, $\overline{\Omega} = \bigcup_{K\in\mathcal{T}_h}\overline{K}$. Let $\mathcal{N}_h = \{\mathbf{x}_\ell\}_{\ell\in L}$ denote the set of all nodes of $\mathcal{T}_h$. We define the finite element spaces

$$V_h := \begin{cases}\big\{\Phi\in C(\overline{\Omega}) : \Phi\big|_K\in P_1(K)\big\} & \text{in the case of for simplices,}\\ \big\{\Phi\in C(\overline{\Omega}) : \Phi\big|_K\in Q_1(K)\big\} & \text{in the case of quadrilaterals/hexaedrals,}\end{cases}$$

$$\overline{\mathbf{V}}_h := [V_h]^d\cap H_0^1(\Omega,\mathbb{R}^d),$$

and the nodal interpolation operator $\mathcal{I}_h : C(\overline{\Omega})\to V_h$, $\mathcal{I}_h\psi = \sum_{\mathbf{z}\in\mathcal{N}_h}\psi(\mathbf{z})\varphi_{\mathbf{z}}$. Here, $\{\varphi_{\mathbf{z}} : \mathbf{z}\in\mathcal{N}_h\}\subset V_h$ denotes the nodal basis for V_h, and $\psi\in C(\overline{\Omega})$. In order to ensure the M-matrix property of the Laplacian we have to distinguish several cases:

(1) triangles: in the case of simplices in two dimensions ($n=2$), we demand that the triangulation $\mathcal{T}_h$ is of acute type, *i.e.*, all angles of any triangle of the triangulation are strictly less than $\pi/2$;
(2) tetrahedrons: in the case of simplices in three dimensions ($n=3$), we also demand $\mathcal{T}_h$ to be of acute type, *i.e.*, all six interior angles of any tetrahedron in the partition are less than $\pi/2$. Although many refinement strategies to not maintain this property of strongly acuteness, there exists a strategy base on so-called 'yellow' triangular elements which maintains this property, see [16];
(3) quadrilaterals: for quadrilateral meshes the theory of the M-matrix property is less investigated. The first work in this direction was carried out by Christie and Hall [4]. They showed examples that the M-matrix property does not hold on arbitrary quadrilateral meshes and give a sufficient condition for rectangular meshes. According to [9], a sufficient condition is that the triangulation consists of non-narrow rectangular meshes. These are meshes consisting of rectangles with the property, that the longest edge of each rectangle is not greater than $\sqrt{2}$ times the shortest one. Furthermore, small 'perturbations' of non-narrow rectangular meshes also fulfill the M-matrix property of the Laplacian but there exist no explicit criteria in the literature.

For $V_h^0 = \big\{\Phi\in V_h : (\Phi,1)=0\big\}$ we introduce the bijective discrete Laplacian $\Delta_h : V_h^0\to V_h^0$ such that

$$(-\Delta_h\Psi,\Phi) = (\nabla\Psi,\nabla\Phi) \qquad \forall\,\Phi\in V_h^0. \tag{4.1}$$

For $\eta\in L^2(\Omega)$ we use the notation $\eta_\Omega := \frac{1}{|\Omega|}(\eta,1)$. The space $L_0^2(\Omega)$ is the standard notation for $\{u\in L^2(\Omega) : u_\Omega = 0\}$. The L^2-projection onto V_h^0 is denoted by $Q_h : L_0^2(\Omega)\to V_h^0$, *i.e.*, $\big(Q_h\psi,\eta\big) = (\psi,\eta)$ for all $\eta\in V_h^0$. Given a time-step size $k>0$, and a sequence $\{\varphi^n\}\subset L^2(\Omega)$, we set $d_t\varphi^n := k^{-1}\{\varphi^n-\varphi^{n-1}\}$ for $n\geq 1$. Note that $(d_t\varphi^n,\varphi^n) = \frac{1}{2}d_t\|\varphi^n\|^2 + \frac{k}{2}\|d_t\varphi^n\|^2$.

The generic constant $C>0$ is independent of solutions $\rho,\mathbf{u}$, and mesh parameters $k,h>0$.

4.2. Finite element based space-time discretization

The advantage of problem (3.11)–(3.14) as a reformulation of (3.1)–(3.5) is that a validation of the energy identity of Lemma 3.1 only requires test functions $(\chi, \mathbf{v}, \xi)$ which are linear functions of the solution $(\rho, \mathbf{u}, w)$. Next to a discretization in space-time of (3.11)–(3.14), the following further concepts are realized in the discrete semi-implicit scheme below to obtain a stable discretization of (2.1)–(2.6) eventually:

(1) the regularization parameters α and γ in the continuity and in the momentum equation, respectively, will be h-dependent;
(2) the truncation parameter β in π'_β will also be h-dependent; moreover $\pi'_\beta(\rho)$ from (3.6) is replaced by its regularization $\widetilde{\pi}_\beta : \mathbb{R} \times \mathbb{R} \to \mathbb{R}$,

$$\widetilde{\pi}_\beta(r_1, r_2) = \begin{cases} \frac{\pi_\beta(r_1) - \pi_\beta(r_2)}{r_1 - r_2} & \text{if } r^1 \neq r^2, \\ \pi'_\beta(r_1) & \text{if } r_1 = r_2, \end{cases} \tag{4.2}$$

where π_β is given in (3.7). This approximation is used to mimic the chain rule in the time-discrete setting;
(3) in the momentum equation, ρ^n in $d_t[\rho^n \mathbf{U}^n]$ will be replaced by the non-negative cut-off function

$$\rho_+^n := \max\{0, \rho^n\}.$$

Later, we will see that $\rho^n = \rho_+^n$, provided that additional assumptions on the choice of α, γ and h are valid. In this case, a cut-off of the density is not necessary.

Scheme $\mathbf{A}^+$: fix $\alpha, \beta, \gamma \geq 0$, and let

$$0 \leq \rho^0 \in V_h, \qquad \text{and} \qquad \mathbf{U}^0 \in \overline{\mathbf{V}}_h.$$

For every $n \geq 1$, find $(\rho^n, w^n, \mathbf{U}^n) \in V_h \times V_h^0 \times \overline{\mathbf{V}}_h$, such that for all $(\chi, \xi, \mathbf{W}) \in V_h \times V_h^0 \times \overline{\mathbf{V}}_h$ holds

$$(d_t \rho^n, \chi) - (\rho^n \mathbf{U}^n, \nabla\chi) + \alpha\big(\nabla\rho^n, \nabla\chi\big) = 0, \tag{4.3}$$

$$\begin{aligned} &\frac{1}{2}\Big((\rho_+^{n-1} d_t \mathbf{U}^n, \mathbf{W}) + (d_t\big[\rho_+^n \mathbf{U}^n\big], \mathbf{W}) + (\rho^{n-1}[\mathbf{U}^{n-1}\cdot\nabla]\mathbf{U}^n, \mathbf{W}) - (\rho^{n-1}[\mathbf{U}^{n-1}\cdot\nabla]\mathbf{W}, \mathbf{U}^n)\Big) \\ &\quad + 2\mu(\mathbf{D}(\mathbf{U}^n), \mathbf{D}(\mathbf{W})) + \lambda(\operatorname{div}\mathbf{U}^n, \operatorname{div}\mathbf{W}) + \gamma(\mathbf{D}(d_t\mathbf{U}^n), \mathbf{D}(\mathbf{W})) + (\rho^n \nabla w^n, \mathbf{W}) = (\rho^{n-1}\mathbf{f}^n, \mathbf{W}), \end{aligned} \tag{4.4}$$

$$\big(w^n, \xi\big) - \Big(\widetilde{\pi}_\beta(\rho^n, \rho^{n-1}), \xi\Big) - \kappa\big(\nabla\rho^n, \nabla\xi\big) = 0. \tag{4.5}$$

Because only the gradient of w enters equation (4.4), it is natural that the mean of w_0 is normalized to zero, *i.e.* $w \in V_h^0$. As will be detailed below, a mild assumption for values k is an essential ingredient to validate existence of iterates by Brouwer's fixed point theorem. Solutions of Scheme A^+ conserve initial mass,

$$\frac{1}{|\Omega|}\int_\Omega \rho^n \,\mathrm{d}\mathbf{x} = \frac{1}{|\Omega|}\int_\Omega \rho^0 \,\mathrm{d}\mathbf{x} =: M_0 \qquad (n \geq 1) \tag{4.6}$$

which follows from (4.3) with $\chi \equiv 1$. Moreover, a discrete energy law involving regularization terms is satisfied.

Theorem 4.1. *Any solution $\big\{(\rho^n, \mathbf{U}^n)\big\}_{n=1}^N \subset V_h \times \overline{\mathbf{V}}_h$ of Scheme A^+ fulfills (4.6), and the following discrete energy identity*

$$\begin{aligned} &d_t\Big[W_{\mathrm{kin}}(\rho_+^n, \mathbf{U}^n) + \widetilde{W}_{VdW,h}(\rho^n, \nabla\rho^n)\Big] + W_{\mathrm{diss}}(\mathbf{U}^n) + kW_{\mathrm{kin}}(\rho_+^{n-1}, d_t\mathbf{U}^n) + \frac{k}{2}\kappa\|\nabla d_t\rho^n\|^2 \\ &+ \alpha\Big[\kappa\|\Delta_h(\rho^n - M_0)\|^2 - \Big(\widetilde{\pi}_\beta(\rho^n, \rho^{n-1}), \Delta_h(\rho^n - M_0)\Big)\Big] + \frac{\gamma}{2}\Big[d_t\|\mathbf{D}(\mathbf{U}^n)\|^2 + k\|\mathbf{D}(d_t\mathbf{U}^n)\|^2\Big] = \big(\mathbf{f}^n, \rho^{n-1}\mathbf{U}^n\big), \end{aligned} \tag{4.7}$$

where $\widetilde{W}_{VdW,h}$ is defined by

$$\widetilde{W}_{VdW,h}(\rho^n, \nabla\rho^n) := \int_\Omega \widetilde{\pi}_\beta(\rho^n)\,\mathrm{d}\mathbf{x} + \frac{\kappa}{2}\,\|\nabla\rho^n\|^2.$$

This result is comparable to Lemma 3.1, apart from the term which involves $\widetilde{\pi}_\beta$, for which we cannot mimic the argument based on the chain rule in the present fully discrete setting, and the two dissipative terms which are weighted by the time step k.

Proof. Choose $\mathbf{W} = \mathbf{U}^n$, and use

$$\begin{aligned}(\rho_+^{n-1} d_t \mathbf{U}^n, \mathbf{U}^n) + (d_t\big[(\rho^n)_+ \mathbf{U}^n\big], \mathbf{U}^n) &= \frac{1}{k}\int_\Omega \Big(\rho_+^n |\mathbf{U}^n|^2 + \rho_+^{n-1}|\mathbf{U}^n|^2 - 2\rho_+^{n-1}\langle \mathbf{U}^{n-1}, \mathbf{U}^n\rangle\Big)\mathrm{d}\mathbf{x}\\ &= \frac{1}{k}\int_\Omega \Big(\rho_+^n |\mathbf{U}^n|^2 + \rho_+^{n-1}|\mathbf{U}^n|^2 + \rho_+^{n-1}\Big[k^2 |d_t\mathbf{U}^n|^2 - |\mathbf{U}^n|^2 - |\mathbf{U}^{n-1}|^2\Big]\Big)\mathrm{d}\mathbf{x}\\ &= \int_\Omega \Big(d_t\big[\rho_+^n |\mathbf{U}^n|^2\big] + k\rho_+^{n-1}|d_t\mathbf{U}^n|^2\Big)\,\mathrm{d}\mathbf{x}\\ &= 2d_t W_{\mathrm{kin}}(\rho_+^n, \mathbf{U}^n) + 2kW_{\mathrm{kin}}(\rho_+^{n-1}, d_t\mathbf{U}^n)\end{aligned}$$

to conclude

$$\begin{aligned}d_t W_{\mathrm{kin}}(\rho_+^n, \mathbf{U}^n) + kW_{\mathrm{kin}}(\rho_+^{n-1}, d_t\mathbf{U}^n) + W_{\mathrm{diss}}(\mathbf{U}^n) +\\ \frac{\gamma}{2}\Big[d_t\|\mathbf{D}(\mathbf{U}^n)\|^2 + k\|\mathbf{D}(d_t\mathbf{U}^n)\|^2\Big] - (\mathrm{div}\big[\rho^n\mathbf{U}^n\big], w^n) - \big(\rho^{n-1}\mathbf{f}^n, \mathbf{U}^n\big) = 0.\end{aligned}$$

In order to reformulate the last-but-one term on the left hand side of this equation, we choose $\chi = w^n$ in (4.3), and $\xi = d_t\rho^n$, resp. $\xi = -\Delta_h(\rho^n - M_0)$ in (4.5). By the discrete version of the chain rule we conclude

$$\begin{aligned}-(\mathrm{div}\big[\rho^n\mathbf{U}^n\big], w^n) &= \big(d_t\rho^n, w^n\big) + \alpha(\nabla[\rho^n - M_0], \nabla w^n)\\ &= d_t\Big(\pi_\beta(\rho^n), 1\Big) + \frac{\kappa}{2}\Big\{d_t\|\nabla\rho^n\|^2 + k\|\nabla d_t\rho^n\|^2\Big\}\\ &\quad + \alpha\Big\{\Big(\widetilde{\pi}_\beta(\rho^n, \rho^{n-1}), -\Delta_h(\rho^n - M_0)\Big) + \kappa\,\|\Delta_h(\rho^n - M_0)\|^2\Big\},\end{aligned} \tag{4.8}$$

thanks to $\alpha\big(\nabla[\rho^n - M_0], \nabla w^n\big) = \alpha\big(-\Delta_h(\rho^n - M_0), w^n\big)$, and (4.1). Putting things together yields (4.7) for solutions of Scheme A^+. □

Remark 4.2. By (3.6), the mean-value theorem, the last terms on the right side of (4.8) may be bounded as follows,

$$\begin{aligned}\alpha\Big[\kappa\|\Delta_h(\rho^n - M_0)\|^2 - \Big(\widetilde{\pi}_\beta(\rho^n, \rho^{n-1}), \Delta_h(\rho^n - M_0)\Big)\Big] &\geq \frac{\kappa\alpha}{2}\|\Delta_h(\rho^n - M_0)\|^2 - \frac{\alpha}{2\kappa}\|\widetilde{\pi}_\beta(\rho^n, \rho^{n-1})\|^2\\ &\geq \frac{\kappa\alpha}{2}\|\Delta_h(\rho^n - M_0)\|^2 - \frac{C}{\kappa}\alpha\beta^2.\end{aligned} \tag{4.9}$$

Putting things together in (4.7), summing up over $1 \leq n \leq N$ yields to ($\mathbf{f} \equiv \mathbf{0}$)

$$\begin{aligned}&\max_{1\leq n\leq N}\Big(W_{\mathrm{kin}}(\rho_+^n, \mathbf{U}^n) + \widetilde{W}_{VdW,h}(\rho^n, \nabla\rho^n)\Big) + k\sum_{n=1}^N \Big(W_{\mathrm{diss}}(\mathbf{U}^n) + kW_{\mathrm{kin}}(\rho_+^{n-1}, d_t\mathbf{U}^n)\Big)\\ &+\frac{k^2}{2}\sum_{n=1}^N\Big(\kappa\,\|\nabla d_t\rho^n\|^2 + \gamma\|\mathbf{D}(\mathbf{U}^n)\|^2\Big) + \frac{\gamma}{2}\max_{1\leq n\leq N}\|\mathbf{D}(\mathbf{U}^n)\|^2 + \frac{\alpha\kappa}{2}k\sum_{n=1}^N\|\Delta_h(\rho^n - M_0)\|^2\\ &\leq W_{\mathrm{kin}}(\rho^0, \mathbf{U}^0) + W_{VdW,h}(\rho^0, \nabla\rho^0) + \left(\frac{\gamma}{2}\|\mathbf{D}(\mathbf{U}^0)\|^2 + \frac{CT}{\kappa}\alpha\beta^2\right).\end{aligned} \tag{4.10}$$

This suggests to balance regularization and truncation *via* $\alpha < \beta^{-2}$, and to choose $h \equiv h(\kappa) > 0$ sufficiently small to reliable control capillarity effects in the numerical scheme.

In order to verify solvability of Scheme A$^+$, we need a preparatory result, which allows to apply Brouwer's fixed point theorem (see *e.g.* [21], p. 37) in step 3 of the proof below.

Lemma 4.3. *Let $n \geq 1$, and $\widehat{\rho}^n := \rho^n - M_0$. Then $(\rho^n, \mathbf{U}^n) \in V_h \times \overline{\mathbf{V}}_h$ solves equation (4.3) if and only if $(\widehat{\rho}^n, \mathbf{U}^n) \in V_h^0 \times \overline{\mathbf{V}}_h$ solves*

$$\Big(\nabla d_t \widehat{\rho}^n, \nabla \xi\Big) - \Big(Q_h \mathrm{div}\big[(\widehat{\rho}^n + M_0)\mathbf{U}^n\big], \Delta_h \xi\Big) + \alpha\big(\Delta_h \widehat{\rho}^n, \Delta_h \xi\big) = 0 \qquad \forall\, \xi \in V_h^0. \tag{4.11}$$

Proof. '$\Rightarrow$'. By definition, for every $\eta \in V_h$, there exists $w \in V_h^0$, such that

$$(\eta, \xi) = \big(\eta - \eta_\Omega + \eta_\Omega, \xi\big) = -\big(\Delta_h w - \eta_\Omega, \xi\big) \qquad \forall\, \xi \in V_h^0.$$

Hence, by (4.6), there holds

$$(d_t \rho^n, \eta) = \Big(d_t[\rho^n - M_0], \eta - \eta_\Omega\Big) \;=\; \Big(d_t[\rho^n - M_0], -\Delta_h w\Big) = \big(\nabla d_t \widehat{\rho}^n, \nabla w\big),$$

and correspondingly, since $\mathrm{div}[\rho^n \mathbf{U}^n] \in L_0^2(\Omega)$, for the same $\eta \in V_h$,

$$\Big(\mathrm{div}[\rho^n \mathbf{U}^n], \eta\Big) = \Big(\mathrm{div}[\rho^n \mathbf{U}^n], \eta - \eta_\Omega\Big) = \Big(Q_h \mathrm{div}\big[(\widehat{\rho}^n + M_0)\mathbf{U}^n\big], -\Delta_h w\Big).$$

Since $\Delta_h w \in V_h^0$,

$$\big(\nabla \rho^n, \nabla \eta\big) = \Big(\nabla[\rho^n - M_0], \nabla[\eta - \eta_\Omega]\Big) = \Big(\Delta_h \widehat{\rho}^n, \Delta_h w\Big).$$

'$\Leftarrow$'. Let $\widehat{\rho}^n \in V_h^0$, then $\rho^n := \widehat{\rho}^n + M_0 \in V_h$. For every $w \in V_h^0$, there exists $\eta \in V_h^0$, such that for every $c \in \mathbb{R}$ holds

$$\Big(\nabla d_t \widehat{\rho}^n, \nabla w\Big) = \Big(d_t[\rho^n - M_0], -\Delta_h w\Big) = \big(d_t \rho^n, \eta - c\big).$$

Correspondingly, by using arguments from the previous step yields for all $c \in \mathbb{R}$, and the definition of $Q_h : L_0^2(\Omega) \to V_h^0$,

$$\big(Q_h \mathrm{div}\big[(\widehat{\rho}^n + M_0)\mathbf{U}^n\big], \Delta_h w\big) = \big(\mathrm{div}[\rho^n \mathbf{U}^n], \eta\big) = \big(\mathrm{div}[\rho^n \mathbf{U}^n], \eta - c\big),$$

as well as

$$\big(\Delta_h[\rho^n - M_0], \Delta_h w\big) = (\nabla \rho^n, \nabla[\eta - c]).$$

This verifies that $\rho^n \in V_h$ solves (4.3) for all $\chi \in V_h$. □

Lemma 4.4. *For arbitrary $\alpha, \gamma \geq 0$, $\beta \geq \beta_0$, arbitrary mesh size $h > 0$, and sufficiently small time steps $k \leq C\kappa\beta^{-2}$ there exists for every $n \geq 1$ a solution $(\rho^n, \mathbf{U}^n) \in V_h \times \overline{\mathbf{V}}_h$ of Scheme A$^+$.*

The proof below studies solvability of the equivalent system (4.12); *cf.* Lemma 4.3. As it turns out, the remaining difficulty is to control the discrete version of the Korteweg terms using boundedness of the π'_β, and the given mesh constraint, which requires proper balancing of space-time discretization parameters with the given $\kappa > 0$.

Proof. By Lemma 4.3, it suffices to study solvability of

$$\begin{aligned}
&\big(\nabla d_t \widehat{\rho}^n, \nabla \xi\big) - \Big(Q_h \mathrm{div}\big[(\widehat{\rho}^n + M_0)\mathbf{U}^n\big], \Delta_h \xi\Big) + \alpha\big(\Delta_h \widehat{\rho}^n, \Delta_h \xi\big) = 0,\\
&\frac{1}{2}\Big\{\Big(\rho_+^{n-1} d_t \mathbf{U}^n, \mathbf{W}\Big) + \Big(d_t\big[(\widehat{\rho}^n + M_0)_+ \mathbf{U}^n\big], \mathbf{W}\Big) + \Big(\rho^{n-1}[\mathbf{U}^{n-1} \cdot \nabla]\mathbf{U}^n, \mathbf{W}\Big)\\
&\qquad - \Big(\rho^{n-1}[\mathbf{U}^{n-1} \cdot \nabla]\mathbf{W}, \mathbf{U}^n\Big)\Big\} + 2\mu\Big(\mathbf{D}(\mathbf{U}^n), \mathbf{D}(\mathbf{W})\Big) + \lambda\Big(\mathrm{div}\,\mathbf{U}^n, \mathrm{div}\,\mathbf{W}\Big)\\
&+ \gamma\Big(\mathbf{D}(d_t \mathbf{U}^n), \mathbf{D}(\mathbf{W})\Big) + \Big(Q_h \mathrm{div}\big[\{\widehat{\rho}^n + M_0\}\mathbf{W}\big], \kappa \Delta_h \widehat{\rho}^n - \widetilde{\pi}_{h^{-\beta}}(\widehat{\rho}^n + M_0, \rho^{n-1})\Big) = \big(\rho^{n-1}\mathbf{f}^n, \mathbf{W}\big),
\end{aligned} \tag{4.12}$$

for all $(\xi,\mathbf{W}) \in V_h^0 \times \overline{\mathbf{V}}_h$. For this purpose, let $n \geq 1$ be fix but arbitrary and define the continuous map

$$\mathbf{F} \equiv [F_1, F_2] : V_h^0 \times \overline{\mathbf{V}}_h \to V_h^0 \times \overline{\mathbf{V}}_h,$$

where for all $(\xi,\mathbf{W}) \in V_h^0 \times \overline{\mathbf{V}}_h$,

$$\begin{aligned}
\Big(F_1\big[\widehat{\rho},\mathbf{U}\big],\xi\Big) &:= \frac{\kappa}{k}\big(\nabla[\widehat{\rho}-\rho^{n-1}],\nabla\xi\big) - \kappa\Big(Q_h\mathrm{div}\big[(\widehat{\rho}+M_0)\mathbf{U}\big],\Delta_h\xi\Big) + \kappa\alpha\big(\Delta_h\widehat{\rho},\Delta_h\xi\big),\\
\Big(F_2\big[\widehat{\rho},\mathbf{U}\big],\mathbf{W}\Big) &:= \frac{1}{2}\Big\{\frac{1}{k}\Big(\rho_+^{n-1}[\mathbf{U}-\mathbf{U}^{n-1}],\mathbf{W}\Big) + \frac{1}{k}\Big((\widehat{\rho}+M_0)_+\mathbf{U}-\rho_+^{n-1}\mathbf{U}^{n-1},\mathbf{W}\Big)\\
&\quad + \Big(\rho^{n-1}[\mathbf{U}^{n-1}\cdot\nabla]\mathbf{U},\mathbf{W}\Big) - \Big(\rho^{n-1}[\mathbf{U}^{n-1}\cdot\nabla]\mathbf{W},\mathbf{U}\Big)\Big\}\\
&\quad + 2\mu\Big(\mathbf{D}(\mathbf{U}),\mathbf{D}(\mathbf{W})\Big) + \lambda\Big(\mathrm{div}\,\mathbf{U}^n,\mathrm{div}\,\mathbf{W}\Big) + \frac{\gamma}{k}\Big(\mathbf{D}(\mathbf{U}-\mathbf{U}^{n-1}),\mathbf{D}(\mathbf{W})\Big)\\
&\quad + \Big(Q_h\mathrm{div}\big[\{\widehat{\rho}+M_0\}\mathbf{W}\big],\kappa\Delta_h\widehat{\rho}-\widetilde{\pi}_{h^{-\beta}}(\widehat{\rho}+M_0,\rho^{n-1})\Big) - \big(\rho^{n-1}\mathbf{f}^n,\mathbf{W}\big).
\end{aligned}$$

We verify existence of a solution for

$$\Big(\mathbf{F}\big[\widehat{\rho}^n,\mathbf{U}^n\big],\big[\xi,\mathbf{W}\big]\Big) = 0 \qquad \forall\,(\xi,\mathbf{W}) \in V_h^0 \times \overline{\mathbf{V}}_h.$$

For this purpose, we compute for all $(\widehat{\rho},\mathbf{U}) \in V_h^0 \times \overline{\mathbf{V}}_h$,

$$\begin{aligned}
\Big(\mathbf{F}[\widehat{\rho},\mathbf{U}],[\widehat{\rho},\mathbf{U}]\Big) &\geq \frac{\kappa}{k}\|\nabla\widehat{\rho}\|\Big(\|\nabla\widehat{\rho}\| - \|\nabla\rho^{n-1}\|\Big) + \kappa\alpha\|\Delta_h\widehat{\rho}\|^2\\
&\quad -\kappa\Big(Q_h\mathrm{div}\big[(\widehat{\rho}+M_0)\mathbf{U}\big],\Delta_h\widehat{\rho}\Big) + \frac{1}{2}\Big\{\frac{1}{k}\|\sqrt{\rho_+^{n-1}}\mathbf{U}\|\Big(\|\sqrt{\rho_+^{n-1}}\mathbf{U}\|\\
&\quad -2\|\sqrt{\rho_+^{n-1}}\mathbf{U}^{n-1}\|\Big) + \frac{1}{k}\|\sqrt{(\widehat{\rho}+M_0)_+}\mathbf{U}\|^2\Big\}\\
&\quad + \Big(Q_h\mathrm{div}\big[(\widehat{\rho}+M_0)\mathbf{U}\big],\kappa\Delta_h\widehat{\rho}\Big) - C\beta\big\|\mathrm{div}\big[(\widehat{\rho}+M_0)\mathbf{U}\big]\big\|_{L^1}\\
&\quad -\|\rho^{n-1}\|\|\mathbf{f}^n\|_{L^\infty}\|\mathbf{U}\| + 2\mu\,\|\mathbf{D}(\mathbf{U})\|^2\\
&\quad +\lambda\,\|\mathrm{div}\,\mathbf{U}\|^2 + \frac{\gamma}{k}\|\mathbf{D}(\mathbf{U})\|\Big(\|\mathbf{D}(\mathbf{U})\| - \|\mathbf{D}(\mathbf{U}^{n-1})\|\Big),
\end{aligned}$$

where the truncation (4.2), the mean-value theorem, and (3.6) are used, as well as the L^1-stability of $Q_h : L_0^2(\Omega) \to V_h^0$; *cf.* [6]. Note that terms three and six on the right-hand side cancel each other. We use the product formula and estimate the remaining term as follows,

$$\begin{aligned}
C\beta\Big(\big\|[\widehat{\rho}+M_0]\mathrm{div}\,\mathbf{U}\big\|_{L^1} + \big\|\langle\nabla\widehat{\rho},\mathbf{U}\rangle\big\|_{L^1}\Big) &\leq C\beta\Big(\|\widehat{\rho}+M_0\|\|\mathrm{div}\,\mathbf{U}\| + \|\mathbf{U}\|\|\nabla\widehat{\rho}\|\Big)\\
&\leq \frac{\lambda}{2}\|\mathrm{div}(\mathbf{U})\|^2 + \mu\|\mathbf{D}(\mathbf{U})\|^2 + C_{\mu,\lambda}\beta^2\Big(M_0 + \|\nabla\widehat{\rho}\|^2\Big).
\end{aligned}$$

For $\|\nabla\widehat{\rho}\| \geq 2\|\nabla\rho^{n-1}\|$, $\|\mathbf{D}(\mathbf{U})\| \geq 2\|\mathbf{D}(\mathbf{U}^{n-1})\|$ and $\|\sqrt{\rho_+^{n-1}}\mathbf{U}\| \geq 2\|\sqrt{\rho_+^{n-1}}\mathbf{U}^{n-1}\|$ we obtain

$$\begin{aligned}
\Big(\mathbf{F}[\widehat{\rho},\mathbf{U}],[\widehat{\rho},\mathbf{U}]\Big) &\geq \kappa\alpha\|\Delta_h\widehat{\rho}\|^2 + \frac{1}{2k}\Big\|\sqrt{(\widehat{\rho}+M_0)_+}\mathbf{U}\Big\|^2 + \mu\,\|\mathbf{D}(\mathbf{U})\|^2 + \frac{\lambda}{2}\,\|\mathrm{div}\,\mathbf{U}\|^2 + \frac{\kappa}{2k}\|\nabla\widehat{\rho}\|^2\\
&\quad + \frac{1}{4k}\Big\|\sqrt{\rho_+^{n-1}}\mathbf{U}\Big\|^2 + \frac{\gamma}{2k}\|\mathbf{D}(\mathbf{U})\|^2 - \|\rho^{n-1}\|\|\mathbf{f}^n\|_{L^\infty}\|\mathbf{U}\| - C_{\mu,\lambda}\beta^2\Big(M_0 + \|\nabla\widehat{\rho}\|^2\Big).
\end{aligned}$$

There exists $C \equiv C(\mu,\lambda) > 0$ such that for all $k \leq C\kappa\beta^{-2}$ we then arrive for $\|\nabla\widehat{\rho}\|$ and $\|\mathbf{D}(\mathbf{U})\|$ sufficiently large at

$$\Big(\mathbf{F}[\widehat{\rho},\mathbf{U}],[\widehat{\rho},\mathbf{U}]\Big) \geq 0.$$

Then, by Brouwer's fixed point theorem [21], page 37, there exists $(\rho^n, \mathbf{U}^n) \in V_h^0 \times \mathbf{V}_h$ such that $\big(\mathbf{F}[\rho^n, \mathbf{U}^n], [\xi, \mathbf{W}]\big) = 0$ for all $(\xi, \mathbf{W}) \in V_h^0 \times \overline{\mathbf{V}}_h$. □

As shown in the previous Lemma, the existence of discrete solutions is independent of the choice of α and γ. However, to show non-negativity of the iterates $\{\rho^n\}$, we need positive values for α and γ. As a consequence, we can replace ρ_+^n, ρ_+^{n-1} in (4.4) by ρ^n, ρ^{n-1}, respectively.

Theorem 4.5. *Let the assumptions of Lemma 4.4 be valid, and $\mathcal{T}_h$ be a triangulation of Ω so that the stiffness matrix of the Laplacian exhibits an M-matrix. Furthermore, we assume the asymptotic relation $\alpha = \alpha(h)$, $\gamma = \gamma(h)$, $\beta = \beta(h)$ complying*

$$0 \;<\; c_1 \left(k^{-1}h^2 + h^{1-d/6}\gamma^{-1/2} \right) \leq \alpha \;\leq\; c_2 \kappa \beta^{-2}\,, \tag{4.13}$$

with constants $c_1, c_2 > 0$ depending on the acuteness of the triangulation. Then $\rho^n = \rho_+^n \geq 0$ for $n \geq 1$.

Proof. We show that for a given $\mathbf{U}^n$ the linear system related to (4.3) exhibits an M-matrix property. We denote the canonical basis of V_h by $\{\varphi_i\}_{i \in I}$ with a finite index set I. For given $\mathbf{U}^n$ equation (4.3) is linear and the corresponding matrix A can be decomposed in the mass matrix M, the Laplacian L, and the convective part K:

$$A = k^{-1}M + \alpha L + K.$$

A sufficient condition for A being an M-matrix is that A is irreducible, weakly diagonal dominant and of non-negative type (*i.e.*, for its coefficients hold $a_{ii} > 0$ and $a_{ij} \leq 0$ for $i \neq j$). This can be shown as follows. Due to the assumption of the used mesh, the Laplacian part L is an M-matrix and fullfils these conditions. Its entries l_{ij} scale as h^{d-2}. Moreover, the mass matrix is always of non-negative type and its entries m_{ij} scale as h^d. The matrix K is indefinite without any M-matrix property. However, the entries of K, denoted by k_{ij}, can be bounded with appropriate constants $c_3, c_4, c_5 > 0$ by

$$k_{ij} \leq c_3 h^{d-1} \|\mathbf{U}^n\|_{L^\infty} \;\leq\; c_4 h^{d-1-d/6} \|\mathbf{U}^n\|_{L^6} \;\leq\; c_5 h^{d-1-d/6} \|\mathbf{D}(\mathbf{U}^n)\|_{L^2},$$

due to the Sobolev's inequality and an inverse estimate. Now, we use the energy estimate (4.10) with $\alpha \lesssim \kappa\beta^{-2}$ and obtain

$$k_{ij} \leq c_6 h^{d-1-d/6} \gamma^{-1/2}.$$

Further, note that for indices i, j with $m_{ij} \neq 0$ of $k_{ij} \neq 0$ it follows $(\nabla\varphi_j, \nabla\varphi_i) \neq 0$ and therefore $l_{ij} \neq 0$. Hence, the upper mentioned sufficient criteria for A being an M-matrix are maintained, if

$$0 < c_1 (k^{-1}h^d + h^{d-1-d/6}\gamma^{-1/2}) \leq \alpha h^{d-2}.$$

This is true due to the assumptions on the parameters. □

Remark 4.6. The M-matrix property of the discrete Laplacian is ensured for triangular meshes (P_1 elements) if the triangulation is of acute type. For rectangular meshes (Q_1 elements) the triangulation should be *e.g. non-narrow*. These are Cartesian grids with the condition that at each rectangle the quotient of the length of the longest edge divided by the shortes one is not larger than $\sqrt{2}$, see [2, 9]. Equidistant tensor grids are of this type. To the authors knowledge, there does not exist a similar result on quadrilateral meshes with hanging nodes.

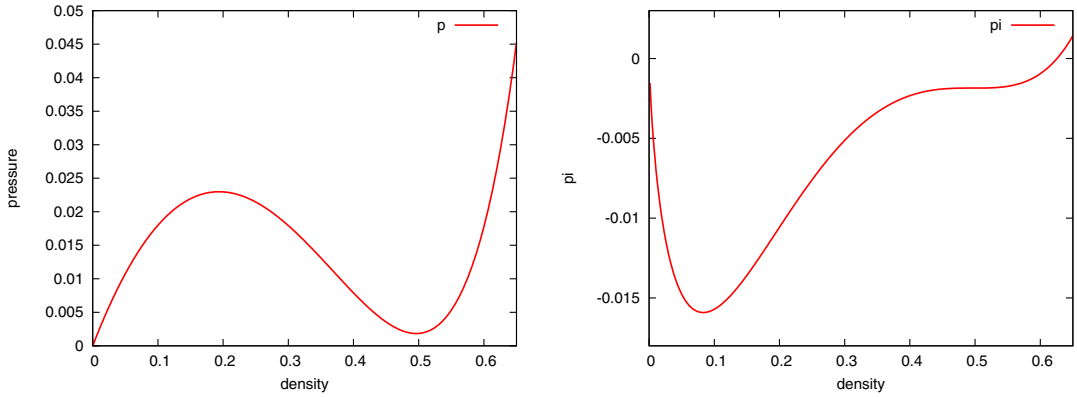

FIGURE 2. Pressure P (left) and potential π (right) in dependence of ρ for the considered setting.

5. Computational studies

The arising discrete system (4.3)–(4.5) is highly coupled and nonlinear. A suitable iterative method for solving such a system is a Newton solver in each time step. Due to the transient computation, the previous time step is a suitable initial guess for starting the Newton iteration. For the arising linear systems we use a geometrical multigrid scheme in order to obtain mesh-size independent convergence rates. However, the design of a robust smoother is not trivial because the corresponding linear systems are non-symmetric and indefinite. That is why we use equal-order finite elements for all variables. This allows us to couple all degrees of freedoms together connected to certain geometrical entities (*e.g.*, for Q_1-elements on each node). This permits us to use a block-ILU smoother within the multigrid iteration.

5.1. 2-D model problem

As numerical model problem we take the configuration suggested by Gomez *et al.* in [11] which describes the coalescence of two bubbles. The computational domain is the two-dimensional unit square $\Omega = (0,1)^2$ and the parameters are

$$\mu \;=\; 1.366 \times 10^{-3}, \quad \kappa \;=\; 10^{-5}, \quad \lambda \;=\; -\frac{2}{3}\mu.$$

The parameters in the algebraic equation for the pressure are chosen as $a = 8 \cdot 0.85/27 = 0.251851852$ and $b = 1$. This choice implies that the fluid temperature is under-critical. Hence, we obtain two phases of the fluid depending on the density. In Figure 2 the pressure and potential π are plotted in dependence of density. The energies π at the densities $\rho_1^* = 0.05$ and $\rho_2^* = 0.65$ are separated by two local minima and one local maximum. The right hand side is set to zero, $\mathbf{f} \equiv \mathbf{0}$. Therefore, due to (2.13), the total energy W of the exact solution should decrease in time. The initial configuration is at rest, $\mathbf{u}_0 \equiv \mathbf{0}$, with non-uniform density distribution:

$$\rho_0 = \rho_1^* + \frac{1}{2}(\rho_2^* - \rho_1^*) \sum_{i=1}^{2} \tanh(100(d_i - r_i))$$

where $d_i = \|\mathbf{x} - \mathbf{x}_i\|$ is the Euclidean distance to the two points $\mathbf{x}_1 = (0.4, 0.5)$ and $\mathbf{x}_2 = (0.78, 0.5)$, and r_i are the radii $r_1 = 0.25$ and $r_2 = 0.1$. The reference density is set to $\overline{\rho} = |\Omega|^{-1} \int_\Omega \rho_0 \, \mathrm{d}\mathbf{x} = 0.48611726$. The initial configuration is shown in Figure 3.

Firstly, the discretization in space is done on equidistant tensor grids by piece-wise bilinear element for all, density, velocity, and the auxiliary variable w. This corresponds to the theoretical investigation in the previous

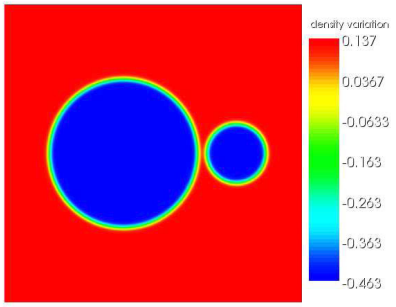

FIGURE 3. Initial density at time $t = 0$. The colors represent the deviation from $\overline{\rho}$.

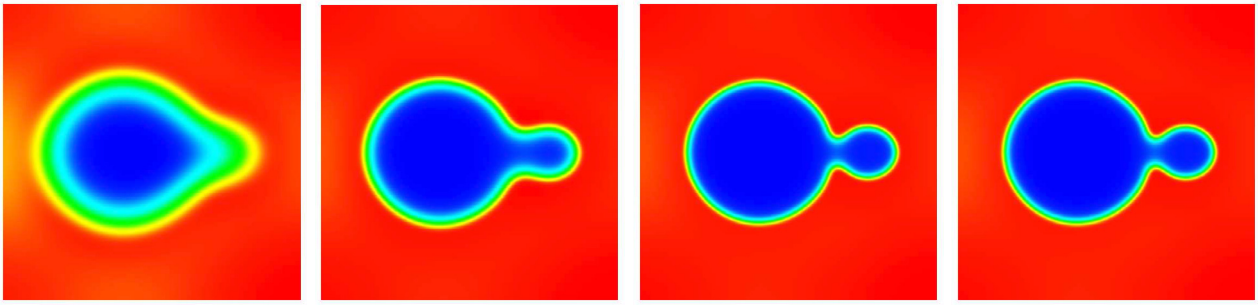

FIGURE 4. Density contour lines at time $t = 0.5$ for different choices of α. The colors represent the deviation from $\overline{\rho} = 0.48611726$. From left to right: $\alpha = h^{2/3}$, $\alpha = h$, $\alpha = h^{4/3}$, $\alpha = h^{3/2}$.

sections. Secondly, to motivate further theoretical studies in this direction, we use locally refined meshes in order to better capture the interface between the two phases. We will see that local mesh refinement also enhances the physical energy decay. We compare the discretization Scheme A^+ for different h-dependences of α. A further stabilization of the convective term was not necessary due to a low Reynolds number and relatively small mesh size, resulting in a low local Peclet number. The time step is always constant $k = 0.05$. In Theorem 4.5, a necessary criterion to ensure non-negativity of computed densities is (4.13), which implies $h^{2/3} \leq \alpha\gamma^{1/2}$. Since the α-regularization introduces numerical diffusion, we are also interested in smaller values of α. Further, since in our experiments the linear and nonlinear systems were always solvable, and densities remain always non-negative, we do not restrict to the criterion in Theorem 4.5. That is why we neglected the entire γ-regularization term and take asymptotically also smaller values of α.

5.2. Results on equidistant tensor meshes

We choose $\alpha = h^a$ with $a \in \{\frac{2}{3}, 1, \frac{4}{3}, \frac{3}{2}, 2\}$. The chosen parameter $\beta > 0$ yields to thresholding values r_β^1 resp. r_β^2 that are smaller resp. larger than the density effectively becomes, such that no truncation occurs, *i.e.* $\pi = \pi_\beta$. This is the reason why no regularization $\pi_\beta(a, b)$ is used in the simulation. Instead, the original potential π and its derivative $\pi'(a)$ were used.

For a comparison we show in Figure 4 the solutions for all choices of the exponent a. Obviously, the scheme is very dispersive for $a \leq 1$ leading to an unphysical vapor phase. For $a = 4/3$ and $a = 1.5$ the interface remains much sharper.

For all choices of α, the overall mass keeps constant and the density remains positive. Let us now consider the total energy W shown in Figure 5 for the different choices of α and different mesh width. For small a (large

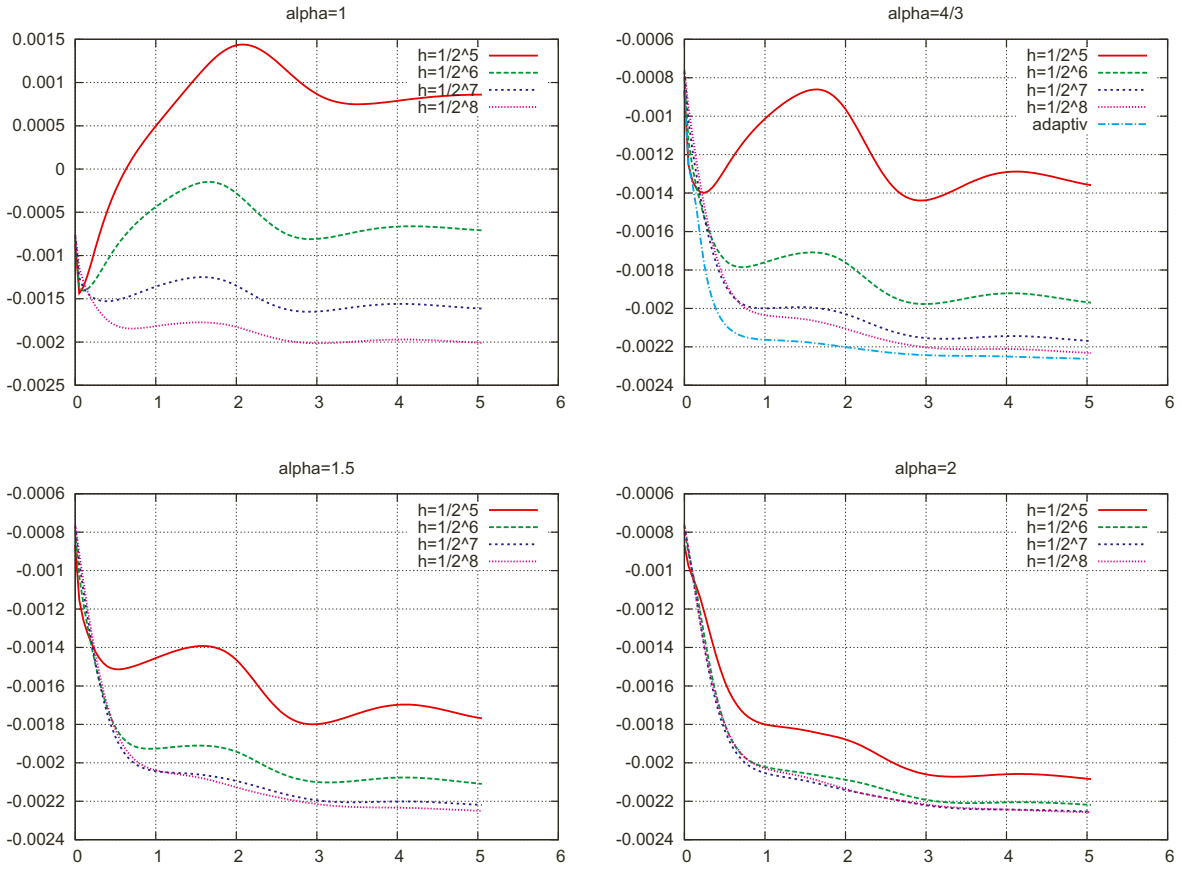

FIGURE 5. Time evolution of the energy $W(t) = W_{\mathrm{kin}}(t) + \widetilde{W}_{VdW,h}(t)$ for different values of $\alpha = h^a$ and different mesh sizes h.

numerical diffusion) the numerical diffusion leads to an unphysical energy rise. For $a = 1$ and coarse meshes an energy rises take place until $t = 2$, and a further (intermediate) rise *e.g.* between $t = 3.5$ and $t = 5$. On finer meshes this (unphysical) phenomena diminishes. For $a \geq 4/3$, the energy always decays on the finest mesh and for $a = 2$ a monotone energy decay takes place on all meshes considered. The artificial energy rise on coarse meshes and for small values a is due to the widened interface which is energetically unfavorable; see Remark 4.2.

In the plot of Figure 6 we show the evolution of the velocity field in the L^2-norm, $\|\mathbf{U}(t)\|$. As explained in [15], the velocity should vanish in the equilibrium, *i.e.* for $t \to \infty$, due to the homogeneous Dirichlet data for $\mathbf{U}$. In the simulations with small values of a and coarse meshes, a rapid decrease of $\|\mathbf{U}(t)\|$ can not be observed. In Table 1, we list the asymptotic values $\lim_{t\to\infty} \|\mathbf{U}(t)\|$ for different values of a and mesh sizes. The fastest decay of the velocity is observed for large values of a and on fine meshes. In Figure 7 streamlines for different time instants are shown. The very right figure shows the remaining velocity field for $t \to \infty$. However, we always observe such parasitic currents, but its magnitude is closely related to a and the mesh size h. For $a = 2$, this velocity field is extremely diminutive ($\|\mathbf{U}(\infty)\| \sim 2.2 \times 10^{-4}$). These simulations again evidence the significance of appropriate choices of α and h in dependence of $\kappa > 0$, and complement the discussion in Remark 4.2: the term considered in (4.9) may be bounded by $\mathcal{O}(\kappa^{-1}\alpha)$ in the present setting, and is only negligible for large choices of a, and a proper resolution in space to account for inherent capillarity effects.

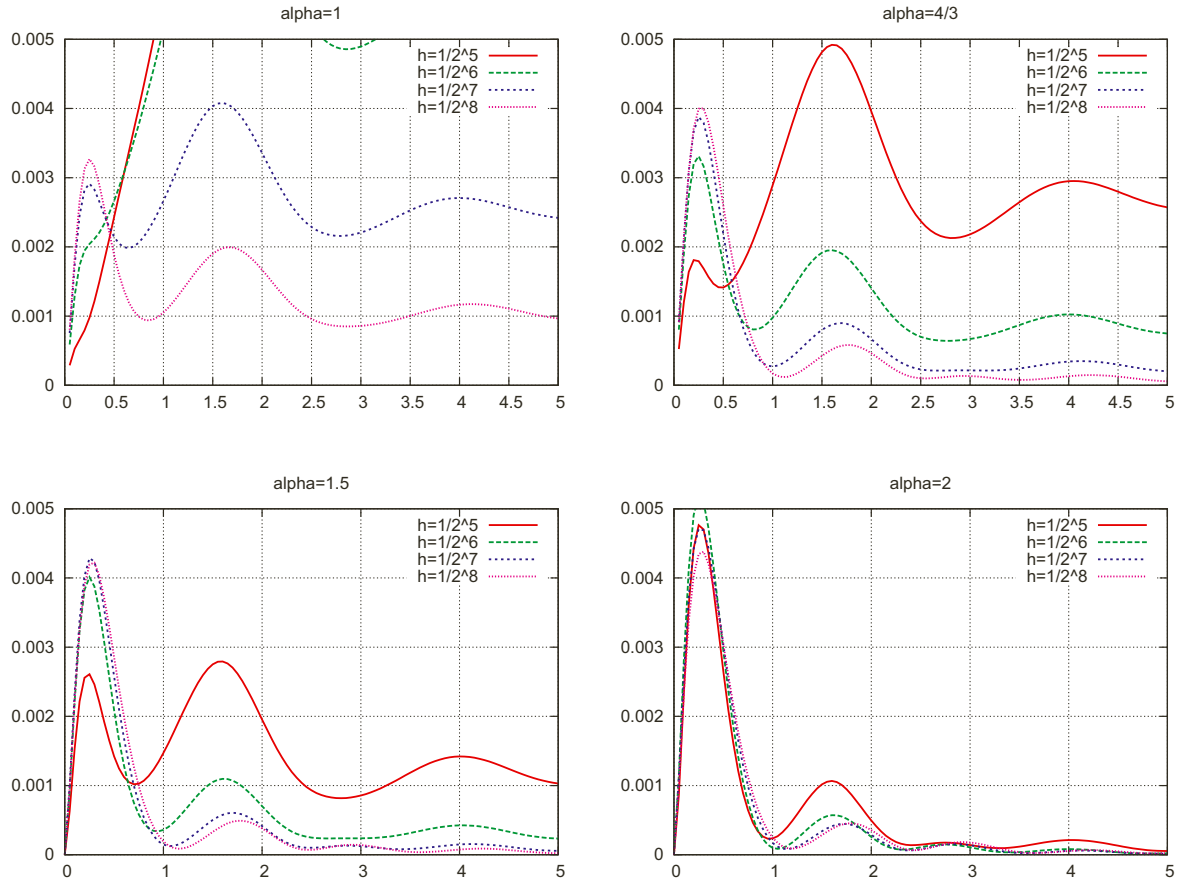

FIGURE 6. Time evolution of the L^2-norm of the velocity field, $\|\mathbf{U}(t)\|^2$, for different values of $\alpha = h^a$. For small a (higher numerical dissipation) this norm velocities does not decrease properly.

TABLE 1. Asymptotic limit $\lim_{t\to\infty} \|\mathbf{U}(t)\|$ for different values of $\alpha = h^a$ and mesh sizes $h = 2^{-l}$. The last row is obtained on an adaptive refined mesh with 29 015 nodes.

l	$a = 1$	$a = 4/3$	$a = 1.5$	$a = 2$
5	1.00e-01	5.12e-01	3.32e-02	7.74e-03
6	7.35e-02	8.91e-02	1.60e-02	2.63e-03
7	4.96e-02	1.45e-02	7.31e-03	8.14e-04
8	3.13e-02	7.16e-03	3.26e-03	2.20e-04
adaptive	2.10e-02	3.27e-03	1.28e-03	5.65e-05

5.3. Results on locally refined meshes

According to Remark 4.2 and the previously shown results on different meshes, one should choose the mesh size h sufficiently small and in dependence on κ. Otherwise a reliable control of capillarity effects is not possible. This is also reflected by this computational study. In the analytical part of this work we considered a uniform

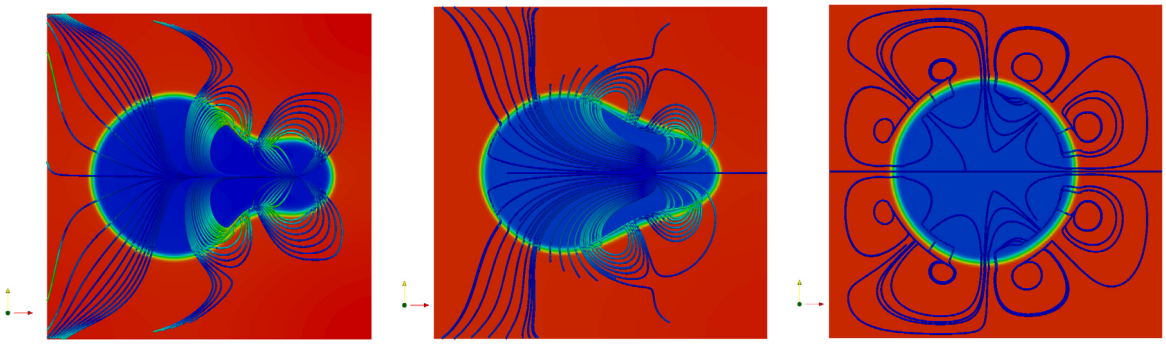

FIGURE 7. Streamlines of the flow with $\alpha = h^2$ at time $t = 2.5$ (left) , $t = 5$ (middle) and for the stationary limit $t \to \infty$ (right). At final time, the flow field exhibits (extremly slowly moving) parasitic currents.

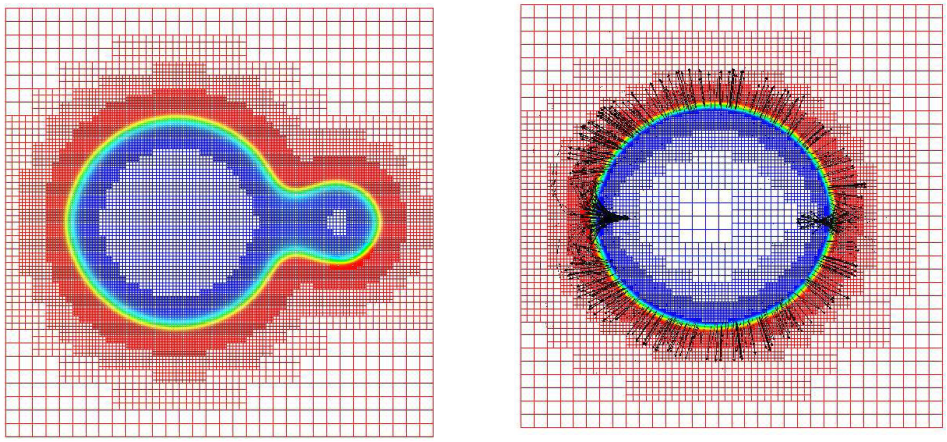

FIGURE 8. Locally refined mesh and density for $\alpha = h^{1.33}$ at $t = 0.5$ (left) and remaining velocity field for $t \to \infty$ (right).

mesh size. However, since small mesh sizes are mainly necessary at the interface, adaptive mesh refinement is a very appropriate method for this kind of problems. Hence, we now employ local mesh refinement in order to reduce the numerical costs without sacrificing a sufficient resolution of the interface. Here, the adaptation criterion is simply based on the jump of the first derivatives across element faces. The number of nodes varies during the transient simulation between $20\,000 < N < 30\,000$. One particular mesh is shown in Figure 8. The corresponding energy curve, shown in Figure 5 (upper right) by the light blue curve, shows that the energy is monotonically decaying. The energy is even lower than the one on a uniform mesh with more degrees of freedom.

5.4. 3-D model problem

Finally we perform a computation with a 3D model. The configuration is the natural extension of the previous two-dimensional model problem into the third dimension. In Figure 9, we show the coalescence of the two bubbles at the two time instants $t = 0.1$ and $t = 0.3$ obtained with the Scheme A+ and $\alpha = h^{4/3}$.

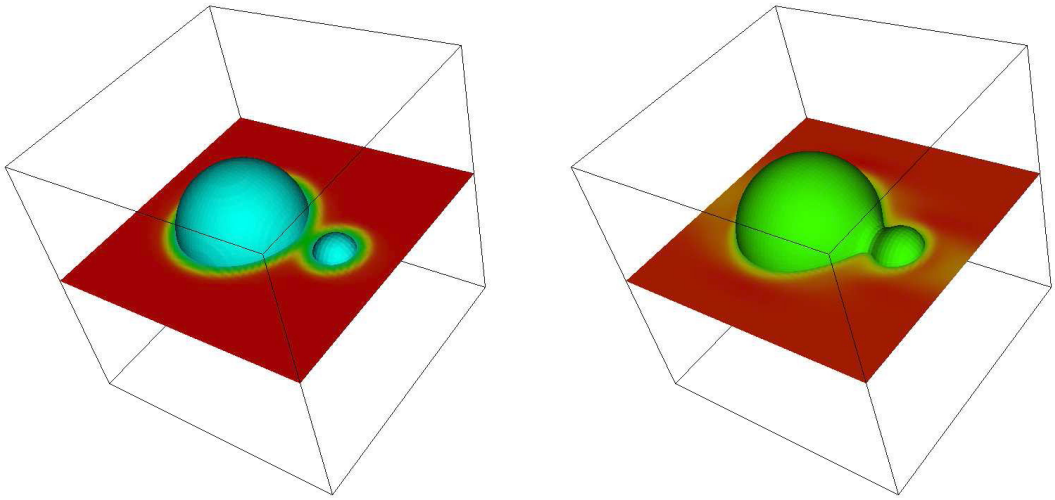

FIGURE 9. Coalescence of two bubbles at the time instants $t = 0.1$ (left) and $t = 0.3$ (right) in three dimensions.

REFERENCES

[1] D.M. Anderson, G.B. McFadden and A.A. Wheeler, Diffuse interface methods in fluid mechanics. *Annu. Rev. Fluid Mech.* **30** (1998) 139–165.

[2] O. Axelsson and V.A. Barker, *Finite Element Solutions of Boundary Value Problems, Theory and Computations*. Academic Press, Inc. (1984).

[3] D. Bresch, B. Desjardins and C.-K. Lin, On some compressible fluid models: Korteweg, lubrication, and shallow water systems. *Commun. Partial Differ. Equ.* **28** (2003) 843–868.

[4] I. Christie and C. Hall, The maximum principle for bilinear elements. *Int. J. Numer. Meth. Eng.* **20** (1984) 549–553.

[5] F. Coquel, D. Diehl, C. Merklea and C. Rohde, Sharp and diffuse interface methods for phase transition problems in liquid-vapour flows, in Numerical methods for hyperbolic and kinetic problems. *IRMA Lect. Math. Theor. Phys.*, Eur. Math. Soc. **7** (2005) 239–270.

[6] M. Crouzeix and V. Thomee, The stability in L^p and W_p^1 of the L^2-projection onto finite element function spaces. *Math. Comput.* **48** (1987) 521–532.

[7] R. Danchin and B. Desjardins, Existence of solutions for compressible fluid models of Korteweg type. *Ann. Inst. Henri Poincaré, Anal. Nonlinear* **18** (2001) 97–133.

[8] J.E. Dunn and J. Serrin, On the thermodynamics of interstitial working. *Arch. Rational Mech. Anal.* **88** (1985) 95–133.

[9] I. Faragó, R. Horváth and S. Korotov, Discrete maximum principle for Galerkin finite element solutions to parabolic problems on rectangular meshes, edited by M. Feistauer *et al.*, Springer. *Numer. Math. Adv. Appl.* (2004) 298–307.

[10] E. Feireisl, *Dynamics of viscous compressible fluids*. Oxford University Press (2004).

[11] H. Gomez, T.J.R. Hughes, X. Nogueira and V.M. Calo, Isogeometric analysis of the isothermal Navier–Stokes–Korteweg equations. *Comput Methods Appl. Mech. Eng.* **199** (2010) 1828–1840.

[12] B. Haspot, Weak solution for compressible fluid models of Korteweg type. `arXiv-preprint server` (2008).

[13] H. Hattori and D. Li, Solutions for two-dimensional system for materials of Korteweg type. *SIAM J. Math. Anal.* **25** (1994) 85–98.

[14] H. Hattori and D. Li, The existence of global solutions to a fluid dynamic model for materials of Korteweg type. *J. Partial Differ. Equ.* **9** (1996) 323–342.

[15] D. Jamet, D. Torres and J.U. Brackbill, On the theory and computation of surface tension: the elimination of parasitic currents through energy conservation in the second-gradient method. *J. Comput. Phys.* **182** (2002) 262–276.

[16] S. Korotov and M. Krizek, Acute type refinements of tetrahedral partitions of polyhedral domains. *SIAM J. Numer. Anal.* **39** (2001) 724–733.

[17] M. Kotschote, Strong solutions for a compressible fluid model of Korteweg type. *Ann. Inst. Henri Poincaré* **25** (2008) 679–696.

[18] C. Liu and N. Walkington, Convergence of numerical approximations of the incompressible Navier–Stokes equations with variable density and viscosity. *SIAM J. Numer. Anal.* **45** 1287–1304 (2007).

[19] C. Rohde, On local and non-local Navier–Stokes–Korteweg systems for liquid-vapour phase transitions. *Z. Angew. Math. Mech.* **85** (2005) 839–857.

[20] R. Scardovelli and S. Zaleski, Direct numerical simulation of free-surface interfacial flow. *Annu. Rev. Fluid Mech.* **31** (1999) 567–603.

[21] R.E. Showalter, *Monotone operators in Banach space and nonlinear partial differential equations*. AMS (1997).